

Analysis of Functional Connectivity Data by Hierarchical Bayesian Models and Applications in Autism Study

**Fei Jie², Rawan A Rupnow¹, Dulal K Bhaumik¹,
Runa Bhaumik¹, Bikas K Sinha³**

¹University of Illinois at Chicago, ²Astellas Pharma, Chicago,
³Indian Statistical Institute, India

Abstract

This article develops a hierarchical Bayesian model for comparing two groups using whole brain functional connectivity data. Significant disrupted connectivities are detected by controlling the false discovery rate. Discoveries identified by the hierarchical Bayesian model are further compared with those detected by the empirical Bayes approach, and a conformity of results is established. Methodological developments are illustrated with a large data set from the Autism Brain Imaging Data Exchange (ABIDE), which includes 361 subjects from 8 medical centers. We observe significantly different functional connectivities involving the Primary Auditory, Visual and Motor Cortices in the autistic group compared to the control group. Multiple hubs of disruptions are also found to inform investigators for possible targets for interventions or development of therapeutic interventions. A potential application of our discoveries is in early detection of subjects who are at high risk of developing neurological disorders.

Keywords: Neuroconnectivity, Functional Magnetic Resonance Imaging, Bayesian Hierarchical Models, False Discovery Rate.

1. Introduction

The human brain is composed of neural populations that work synchronously via various forms of connections to perform cognitive tasks. A failure at any component in the human brain system results in improper function of tasks. A detailed understanding of brain disruptions in neurological conditions is fundamental to the development of treatments for these diseases. To this end, numerous efforts have been made to decipher the relationship between neurological conditions and changes in brain connectivity. For example, the Human Connectome Project (<http://www.humanconnectomeproject.org/>) represents the most ambitious effort to map the neural pathways that underlie the function of the human brain.

This effort will pave the way toward a better understanding of how brain connectivity is involved in the pathophysiology of aging and disease. Similarly, the 1000 Functional Connectome Project is the largest repository of fMRI data for studying autism. Autism is a neurodevelopmental disorder that is characterized by poor social communication abilities, repetitive behaviors, or restricted interests. This broad classification includes autistic disorder, Asperger syndrome, and pervasive developmental disorder not otherwise specified (PPD-NOS) according to DSM-IV [2]. As this is an etiologically and clinically diverse group of disorders, it is commonly referred to as the autism spectrum disorders (ASD). It is estimated that ASD strikes 1-2 per 1000 people [8], making it of the utmost importance for research to elucidate its etiology.

Neural connectivity usually refers to a pattern of anatomical links (structural connectivity) and statistical dependencies (functional connectivity). Functional connectivity is defined as the temporal dependence of activities of anatomically separated regions of the brain [1, 9]. It may similarly be described as synchronized and correlated patterns of activity that can even occur between pairs of structurally unconnected regions. Functional magnetic resonance imaging or functional MRI (fMRI) is a neuroimaging procedure that measures brain activity by detecting associated changes in blood flow. fMRI has become a dominant neuroimaging technique; in fact, it played a critical role in establishing ASD as a neurological disorder. fMRI measures brain activity using blood oxygen-level dependent (BOLD) response, a function of changes in the amount of deoxyhemoglobin in the tissue. Functional connectivity is then characterized from fMRI data by similar activation patterns of anatomically separated regions, indicating functional communications, or links, between these regions. Due to its excellent contrast properties, spatial resolution, and temporal resolution, fMRI is ideally suited for autism research. Additionally, it is non-invasive and does not need radio-labeling, making it a relatively simple technique to administer to patients.

Statistical analysis of functional connectivity data to study autism spectrum disorder needs to be given special attention, as multidimensional complexities, such as within subject variability, between subject heterogeneity and study site variations are present in such data. Detection of disrupted connectivities of autistic subjects compared to healthy controls is often one of the main goals of such studies. In whole brain studies, where thousands of links are measured, discovering true disruptions becomes challenging as false discoveries often derail the process. Controlling the number of false discoveries is a critically important step, as otherwise further research and effort is wasted on incorrect conclusions. Thus, appropriate modeling of such data together with the implementation of a

proper multiple testing procedure to control false discoveries is extremely important in search for true disruptions.

In this article, we develop a hierarchical Bayesian model to analyze resting state functional neuroconnectivity data. Our primary goal is to develop and apply the proposed statistical methods to neuroconnectivity data for comparing subjects having neurological conditions (e.g., autism, psychiatric etc.) with healthy controls to identify disrupted connectivities for application of better therapeutic interventions. We also identify hubs of disrupted neuroconnectivities, which are critically important for classifying subjects falling in a high-risk category to prevent future catastrophes, such as suicide ideation or complete suicide. In search of disrupted connectivities, we aim to prevent false discoveries. The most common approach to controlling the type I error rate is inappropriate for multiple testing of correlated hypotheses in fMRI data. Thus, proper analysis requires an innovative approach to control the false discovery rate in this setting. Our proposed approach provides a second layer of confidence in diagnosing neurological disorders, as it based on functional connectivity measures which further can be correlated with neurobehavioral measures as opposed to neurobehavioral measures only.

We organize the article as follows. In Section 2, we motivate our problem with a study related to autism spectrum disorders (ASD). In Section 3, we develop a Bayesian model, particularly suitable for our study design and apply a multiple testing procedure to control false discoveries. We perform a simulation study and show satisfactory performance of our proposed model in Section 4. We then apply our approach to the Autism Brain Imaging Data Exchange (ABIDE) for identifying disrupted links. The conclusion is presented in Section 5.

2. Motivational Example: Autism Brain Imaging Data Exchange

We illustrate our approach using fMRI measures from the Autism Brain Imaging Data Exchange, which is part of the 1000 Functional Connectome Project/International Neuroimaging Data-sharing Initiative (INDI) (http://fcon_1000.projects.nitrc.org/). This exchange is the largest repository of fMRI data for autism, consisting of 16 sites among medical centers around the globe. It consists of 1112 datasets of fMRI data and phenotypic information for 539 autism patients and 573 typically developing controls. All datasets in ABIDE are fully anonymized to be consistent with HIPAA (Health Insurance Portability and Accountability) guidelines and 1000 Functional Connectomes Project / INDI protocols. Detailed information regarding sample size, subject characteristics

(e.g., age), diagnostic criteria, data acquisition, and site-specific protocols at each medical center can be found at: http://fcon_1000.projects.nitrc.org/indi/abide/. The data was preprocessed by the Connectome Computation System (CCS) pipeline, as described at <http://preprocessed-connectomes-project.org/abide/ccs.html>.

In this article, we use fMRI measurements from 8 participating sites. The number of subjects at each site is summarized in Table 1. Most of the sites have fewer than 60 subjects, except for NYU. In total, we have 361 subjects, which consists of 189 controls and 172 autistic subjects. We choose to work with the 84 Brodmann Regions of the ABIDE datasets. A list of all regions with numbers is given in Table 2. With 84 regions of measurements, a total of $(84 \times 83)/2 = 3486$ links are involved. A 3486×3486 matrix of Fisher transformed Pearson correlation coefficients were obtained for each subject from the ROI time courses. This represents an association matrix of functional connectivity between all possible pairs of ROIs.

Table 1. Number of Subjects at Each Site

Site	Control	Autism	Total
Caltech	21	16	37
NYU	42	35	77
Olin	16	20	36
Pitt	28	30	58
SBL	15	15	30
SDSU	22	14	36
SJH	25	22	47
Stanford	20	20	40
Total	189	172	361

3. Methods

In this section, we discuss and develop statistical methodologies for detecting disrupted connectivities in group comparison studies.

3.1 Hierarchical Bayesian Model

Bayesian statistics has become extremely useful for data analysis, and is now considered a viable alternative to classical frequentist theory. The term

hierarchical Bayes was introduced by Good in 1965 [13]. In recent years, hierarchical Bayesian modeling has been very useful in modeling complex problems with multiple parameters. Assume observations y_{ij} are grouped into m clusters: $y_{11}, \dots, y_{1n_1}; y_{21}, \dots, y_{2n_2}; \dots; y_{m1}, \dots, y_{mn_m}$. Hierarchical models assume $y_{ij} \sim f(y|\theta_i), j = 1, \dots, n_i, i = 1, \dots, m$ and $\theta_1, \dots, \theta_m$ are iid with distribution $\pi(\theta|\eta)$.

In many statistical applications, data are correlated or connected in a certain pattern. Hierarchical models allow the assessment of the within and between cluster effects. Furthermore, non-hierarchical models are usually not suitable for hierarchical data due to the difficulty in identifying the correct number of parameters.

The implementation of hierarchical Bayesian modeling requires computational power. For illustration, suppose the study data has the following hierarchical structure:

$$Y_i \sim \text{Normal}(\mu, \sigma^2),$$

$$\mu, \sigma^2 \sim \pi(\mu, \sigma^2),$$

Table 2. Regions Analyzed

Region Number (Odd=Left, Even=Right)	Region Description
01,02	BA.1 Primary Somatosensory Cortex
03,04	BA.10 Anterior Prefrontal Cortex
05,06	BA.11 Orbitofrontal Cortex
07,08	BA.13 Insular Cortex
09,10	BA.17 Primary Visual Cortex
11,12	BA.18 Secondary Visual Cortex
13,14	BA.19 Associative Visual Cortex
15,16	BA.2 Primary Somatosensory Cortex
17,18	BA.20 Inferior Temporal Gyrus
19,20	BA.21 Middle Temporal Gyrus
21,22	BA.22 Superior Temporal Gyrus
23,24	BA.23 Ventral Posterior Cingulate Cortex
25,26	BA.24 Ventral Anterior Cingulate Cortex
27,28	BA.25 Subgenual cortex
29,30	BA.27 Piriform Cortex
31,32	BA.28 Posterior Entorhinal Cortex

33,34	BA.29 Retrosplenial Cingulate Cortex
35,36	BA.3 Primary Somatosensory Cortex
37,38	BA.30 Cingulate Cortex
39,40	BA.31 Dorsal Posterior Cingulate Cortex
41,42	BA.32 Dorsal Anterior Cingulate Cortex
43,44	BA.33 Anterior Cingulate Cortex
45,46	BA.34 Anterior Entorhinal Cortex
47,48	BA.35 Perirhinal Cortex
49,50	BA.36 Parahippocampal Cortex
51,52	BA.37 Fusiform Gyrus
53,54	BA.38 Temporopolar Area
55,56	BA.39 Angular Gyrus
57,58	BA.4 Primary Motor Cortex
59,60	BA.40 Supramarginal Gyrus
61,62	BA.41 Primary Auditory Cortex
63,64	BA.42 Primary Auditory Cortex
65,66	BA.43 Subcentral Area
67,68	BA.44 IFC Pars Opercularis
69,70	BA.45 IFC Pars Triangularis
71,72	BA.46 Dorsolateral Prefrontal Cortex
73,74	BA.47 Inferior Prefrontal Gyrus
75,76	BA.5 Somatosensory Association Cortex
77,78	BA.6 Premotor Cortex
79,80	BA.7 Somatosensory Association Cortex
81,82	BA.8 Dorsal Frontal Cortex
83,84	BA.9 Dorsolateral Prefrontal Cortex

where $\pi(\mu, \sigma^2)$ is the joint prior distribution of μ and σ^2 .

By Bayes theorem, the joint posterior distribution $\pi(\mu, \sigma^2 | Y)$ of μ and σ^2 is given by:

$$\pi(\mu, \sigma^2 | Y) \propto L(\mu, \sigma^2) \pi(\mu, \sigma^2)$$

where $L(\mu, \sigma^2)$ is the likelihood of μ and σ^2 . However, for statistical inference, the marginal posterior is needed. To derive the marginal posterior distribution of a parameter, one needs to integrate out all other parameters from the joint posterior distribution. In this example, the two marginal posterior distributions can be expressed as:

$$f(\mu|Y) = \int \pi(\mu, \sigma^2|Y) d\sigma^2$$

$$f(\sigma^2|Y) = \int \pi(\mu, \sigma^2|Y) d\mu$$

When there is a much larger number of second-level parameters to be estimated, this algorithm is not nearly as simple. This problem of high dimensional integration was generally a formidable analytic problem which had hindered the application of hierarchical Bayesian analysis until the late 1980s. See [5] for an excellent review.

3.2 Implementation of Hierarchical Bayesian Model

Implementation of a hierarchical Bayesian model was historically a challenging task due to high-dimensional integration. However, the advancement of computational tools in recent years makes it possible to sample from the marginal posterior distributions of high-dimensional parameters. Most of these techniques are based on Markov chain Monte Carlo, which we briefly describe below with an algorithm for implementation.

3.2.1 Markov Chain Monte Carlo

Markov chain Monte Carlo (MCMC) is a computational tool that can be used to sample from posterior distributions. It was first introduced by Metropolis in 1953 [16]. Later developments include Hasting's generalization of Metropolis' algorithm [14] and the invention of the Gibbs sampler by [11]. Markov chain Monte Carlo was rediscovered by Bayesian scientists in the late 1980s. Over the years, MCMC has become popular in Bayesian computational statistics and has made significant contributions to the propagation of Bayesian theory. The central idea of MCMC is to construct a Markov chain whose stationary distribution is the target distribution. MCMC produces dependent samples as it is an iterative procedure.

A Markov chain is a stochastic process $\theta^{(1)}, \theta^{(2)}, \dots, \theta^{(t)}, \dots$ such that

$$f(\theta^{(t+1)}|\theta^{(1)}, \theta^{(2)}, \dots, \theta^{(t)}) = f(\theta^{(t+1)}|\theta^{(t)}) \forall t.$$

The distribution of θ at time point $t + 1$ given the values of all previous time points depends only the value at the immediate previous time point (i.e., $\theta^{(t)}$). In addition, $f(\theta^{(t+1)}|\theta^{(t)})$ is independent of time t . Lastly, under certain conditions,

the distribution of $\theta^{(t)}$ converges to its equilibrium distribution. This convergence is independent of the choice of initial values $\theta^{(0)}$.

The Markov chain needs to converge to the target posterior distribution before sampling is performed. In addition, it should be easy to sample from the conditional distribution $f(\theta^{(t+1)}|\theta^{(t)})$. Assuming the Markov chain satisfies the above-mentioned conditions, the MCMC algorithm can be summarized as follows:

1. Choose an initial value $\theta^{(0)}$ for the Markov chain(s).
2. Generate T values (iterations) until the chain(s) reaches equilibrium.
3. Evaluate convergence of the algorithm by examining convergence diagnostics. If the diagnostics fail, generate more observations.
4. Remove the first B observations (i.e., burn-in process).
5. Use the remaining $T - B$ values $\theta^{(B+1)}, \dots, \theta^{(T)}$ as posterior samples.
6. Obtain the summary statistics of the posterior sample (e.g. mean, standard deviation, quantiles, correlations). Perform Bayesian inferences using these posterior samples.

After posterior samples of $\theta, \theta^{(1)}, \dots, \theta^{(T)}$, are obtained, statistical inferences can be made on any function of θ , say $G(\theta)$. The algorithm is as follows (see [18]):

1. Obtain a sample of $G(\theta)$ of size T by plugging in $\theta^{(1)}, \dots, \theta^{(T)}$.
2. Obtain summary statistics of $G(\theta)$ using traditional sample estimates. For instance, the posterior mean of $G(\theta)$ can be approximated by $\frac{1}{T} \sum_{t=1}^T G(\theta^{(t)})$. Similarly, one can derive other quantities such as the posterior standard deviation, median or quantiles of $G(\theta)$.

3.2.2 Metropolis-Hasting Algorithm

Since Metropolis first introduced the MCMC method, there have been several developments in expanding the original method. These include the Metropolis-Hasting algorithm, Gibbs sampler, slice sampler, reversible jump MCMC and perfect sampling. Most of the later developments are more complicated than the original Metropolis algorithm and focus on specific problems. The main idea behind the Metropolis algorithm is a random walk that uses an acceptance/rejection rule to converge to the target distribution. The steps for drawing samples from the posterior distribution $p(\theta|y)$ can be summarized as follows:

1. Identify a jumping density $J_t(\theta^*|\theta^{t-1})$. The jumping density must be symmetric, i.e. $J_t(\theta_a|\theta_b) = J_t(\theta_b|\theta_a)$.
2. Draw θ^* from $J_t(\theta^*|\theta^{t-1})$.
3. Compute the ratio $r = \frac{p(\theta^*|y)}{p(\theta^{t-1}|y)}$.
4. If $r \geq 1$, set θ^t to θ^* . Otherwise set θ^t to θ^{t-1} with probability r and θ^{t-1} with probability $1 - r$.

Metropolis' method was generalized to what is known as the Metropolis-Hasting algorithm [14]. The main improvements include (1) the jumping density does not need to be symmetric, and (2) the ratio r is replaced by

$$r = \frac{\frac{p(\theta^*|y)}{J(\theta^*|\theta^{t-1})}}{\frac{p(\theta^{t-1}|y)}{J(\theta^{t-1}|\theta^*)}}$$

3.2.3 Gibbs Sampler

Gibbs sampler was developed in [11] as a special case of Metropolis-Hasting. Suppose θ consists of d components, $\theta = (\theta_1, \theta_2, \dots, \theta_d)$. Then, each iteration of Gibbs sampler consists of a series of d steps. In step j of iteration t , Gibbs sampler utilizes the full conditional posterior distribution

$$p(\theta_j|\theta_{-j}^{t-1}, y)$$

to update θ_j , where θ_{-j}^{t-1} represents all components of θ except for θ_j :

$$\theta_{-j}^{t-1} = (\theta_1^t, \theta_1^t, \dots, \theta_{j-1}^t, \theta_{j+1}^t, \dots, \theta_d^t).$$

The algorithm of Gibbs sampler can be summarized as follows:

1. Set initial values $\theta^{(0)}$.
2. For $t = 1, \dots, T$, repeat the following steps:
 - a. Set $\theta^{(t)} = \theta^{(t-1)}$.
 - b. For $j = 1, \dots, d$, update θ_j from $\theta_j \sim p(\theta_1^t, \theta_1^t, \dots, \theta_{j-1}^t, \theta_{j+1}^t, \dots, \theta_d^t, y)$.
 - c. Set $\theta^{(t)} = \theta$ and save it as the generated sample at iteration $t + 1$.

Gibbs sampler has been very popular since it only requires sampling from univariate distributions. Many statistical packages such as R and SAS provide standard functions that can easily generate random numbers from univariate distributions. WinBUGS is a free software that generates random numbers from posterior distribution of parameters in Bayesian models. It was developed by

statisticians in the Medical Research Council Biostatistics Unit in University of Cambridge. The original version, which was developed on the UNIX platform, is called BUGS, or Bayesian inference Using Gibbs Sampler. As WinBUGS implements Gibbs sampler, it allows for sampling sequentially from each parameter's full conditional distribution.

4. Data Analysis Using Bayesian Hierarchical Model

4.1 Model Specification

The joint distribution of data and parameters in a hierarchical model can be expressed as

$$f(y|\theta_1)\pi_1(\theta_1|\theta_2)\pi_2(\theta_2|\theta_3) \dots \pi_k(\theta_k|\lambda)$$

where $f(y|\theta_1)$, $\pi_1(\theta_1|\theta_2)$, ..., $\pi_k(\theta_k|\lambda)$ specify the first, second, ..., k^{th} level of the hierarchical model, respectively. The main interest is usually in the marginal posterior distribution of first level parameters, $p(\theta_1|y)$. This can be obtained by Gibbs sampling via WinBUGS after the hierarchical model is specified. To fit the Bayesian hierarchical model to our fMRI data, the first level of the model is the mixed-effects model described below:

$$Y_{ij} = \beta_{0i} \times (1 - G_j) + \beta_{1i} \times G_j + \gamma_j + \varepsilon_{ij},$$

where Y_{ij} is the fMRI measurement for the i^{th} link from the j^{th} subject, $i = 1, \dots, m$ and $j = 1, \dots, n$. In this study, there are $m = 3486$ links. $G_j = 0$ for control subjects while $G_j = 1$ if the subject is from the autism group. γ_j is the random effect term for the j^{th} subject and ε_{ij} is the error term. We assume that $\gamma_j \sim N(0, \sigma_\gamma^2)$, where $\gamma_1, \dots, \gamma_n$ are independent. Furthermore, $\varepsilon_{ij} \sim N(0, \sigma_{0i}^2)$ for control group subjects, $\varepsilon_{ij} \sim N(0, \sigma_{1i}^2)$ for autistic subjects, and all ε_{ij} are independent. Moreover, γ_j is assumed to be independent of ε_{ij} .

The fMRI measurement for the i^{th} link given the subject effect γ can be modeled as

$$Y_{ij}|\gamma_j \sim N(\beta_{0i} + \gamma_j, \sigma_{0i}^2)$$

for subjects in the control group and

$$Y_{ij}|\gamma_j \sim N(\beta_{1i} + \gamma_j, \sigma_{1i}^2)$$

for subjects in the autism group. We also assume that

$$\beta_i = \begin{bmatrix} \beta_{0i} \\ \beta_{1i} \end{bmatrix} \sim N \left(\begin{bmatrix} 0 \\ 0 \end{bmatrix}, \begin{bmatrix} \sigma_{\beta_{0i}}^2 & 0 \\ 0 & \sigma_{\beta_{1i}}^2 \end{bmatrix} \right).$$

Without any prior knowledge of model parameters, we assign the following values to the hyperparameters so that the priors contain almost no information:

$$\sigma_{\beta_{0i}}^2 = 1000, \sigma_{\beta_{1i}}^2 = 1000, \sigma_{\sigma_{0i}}^2 = 1000, \sigma_{\sigma_{1i}}^2 = 1000, \sigma_{\gamma}^2 = 1000.$$

To detect disrupted links, we test the null hypothesis $H_0: \beta_{1i} = \beta_{0i}$ for $i = 1, \dots, m$.

4.2 Model Update and Diagnosis

In this section, we describe how we update our models and provide diagnostics tests for convergence. The goal of WinBUGS analysis is to draw samples from corresponding posterior distributions. It is crucial to check the convergence of underlying results. However, since the posterior distribution has an unknown nonstandard form in most cases, convergence cannot be proved immediately. It is customary to run diagnostic tests to evaluate whether WinBUGS has converged to a stationary distribution. As a single test cannot guarantee convergence, it is recommended to run more than one test. For this purpose, we use a test based on the Brooks-Gelman-Rubin (bgr) test ([10], [4]) and Geweke test. The original Gelman-Rubin diagnostics test was a univariate statistic, referred to as the potential scale reduction factor, or PSRF. The idea behind the ANOVA-type diagnostic is that when chains converge to the target distribution, the between chain variation should become small relative to the within chain variation, yielding a PSRF close to 1.

The PSRF was later extended to a new test that can simultaneously assess the convergence of multiple parameters in the form of a multivariate potential scale reduction factor (MPSRF). The relationship between PSRF and MPSRF can be expressed as

$$\max \text{PSRF}_i \leq \text{MPSRF}.$$

A rule of thumb for non-convergence is 0.975 quantile of MPSRF larger than 1.2. In Geweke's test, the convergence of each chain can be examined by viewing the set of values simulated by MCMC as a time series [12]. The mean from earlier segments of the chain is compared to the mean in a later segment. A z-test is applied to check whether these two means are equal. If the hypothesis that the means at the beginning and the end of the MCMC output are equal is rejected, then the convergence of the chain cannot be assumed.

As WinBUGS relies on Gibbs sampling to generate random numbers from posterior distribution, it samples sequentially from each parameter's full conditional distribution. Due to the sequential nature of the MCMC algorithm, WinBUGS produces correlated samples from the true joint posterior distribution. We monitor the correlation between neighboring draws to make sure that the algorithm is stopped at the right iteration.

4.3 Analysis Results

We preprocessed fMRI data in R and then fed it into WinBUGS using R2WinBUGS package. The mixed-effects model is fitted in WinBUGS. We chose to run 3 chains for 1100 iterations with a burn-in of the first 1000 iterations to obtain 300 sets of samples. Convergence is assessed using both the Gelman test and Geweke test.

Table 3: Geweke Diagnostics Test

Variable Name	Geweke Value
sigma1[3476]	-4.045e-01
sigma1[3477]	-1.142e00
sigma1[3478]	5.833e-01
sigma1[3479]	-4.976e01
sigma1[3480]	8.869e-01
sigma1[3481]	1.035e00
sigma1[3482]	6.336e01
sigma1[3483]	-9.782e-02
sigma1[3484]	7.883e-01
sigma1[3485]	-3.489e-01
sigma1[3486]	-3.351e-01

Part of the output from the Geweke diagnostics test is listed in Table 3. The mean of the first 10% samples are compared with the last 50% samples in the Z score calculation. Since the Z statistic only applies to a single chain, the test is applied separately to each of the three chains. The z scores from all three chains are not significant at the 0.05 level, indicating no evidence of deviation from

convergence. The BGR diagnostic was also obtained via the CODA package. PSRF does not provide evidence of deviation from convergence as 0.975 quantiles are all less than 1.2. Moreover, MPSRF is equal to 1, which confirms that MCMC has converged. Convergence is further investigated graphically via trace-plots that display a time series plot of individual sampled for individual parameter in each chain. The trace-plots for several parameters in our model is presented in Figure 1(a). All the values are within a zone without apparent periodicities, validating our assumption that convergence has been achieved. In addition, the density plots have a nice bell-shape, which is consistent with the posterior normal distribution.

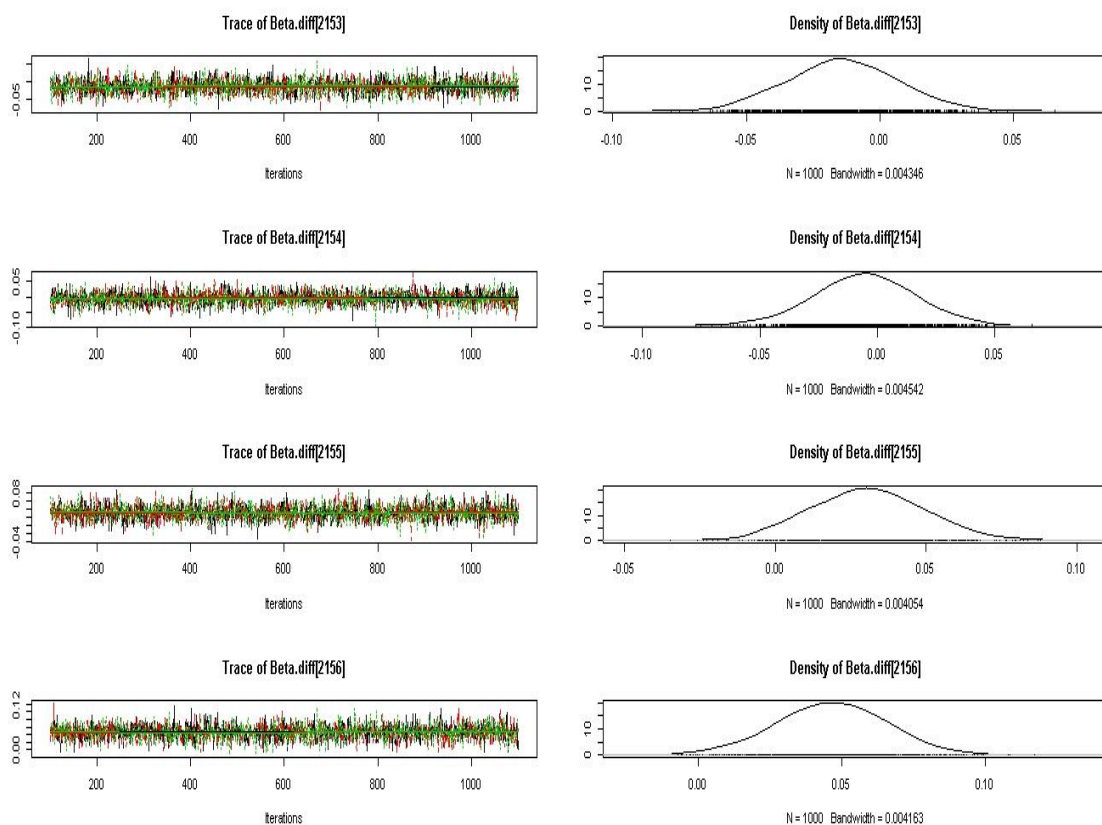


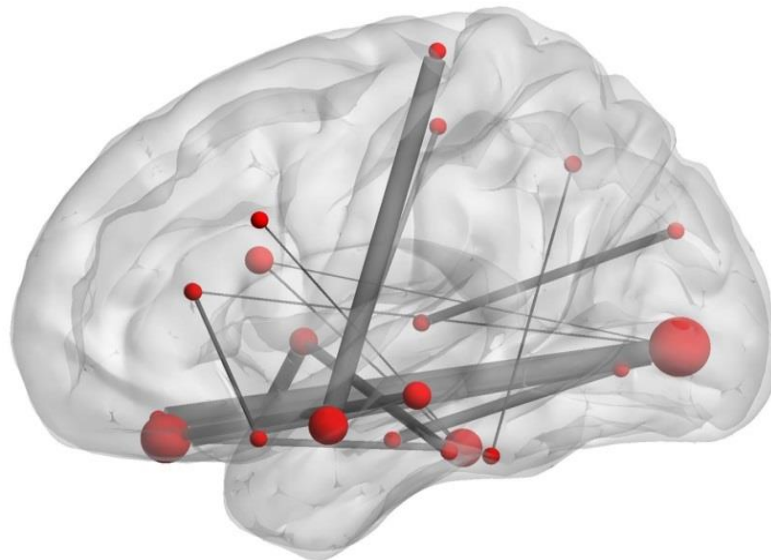
Figure 1: Diagnostics Plots (a) Trace Plot (b) Density Plot

Once convergence is confirmed via multiple tests and graphical tools, analysis

was performed in WinBUGS and the FDR approach implemented due to multiple-testing. To control the false discovery rate in multiple testing, we used Benjamini Hochberg approach [3] with a false discovery rate of .30. Links with significant difference between autism and control subjects are presented in Table 4. Inspecting Table 4, we see that a total of 17 connectivities are found to be significant. Figure 2 is a brain network plot that depicts the 17 significant links.

4.4 Hierarchical Bayesian Results vs Empirical Bayesian Results

We further compared Hierarchical Bayesian (HB) results with those detected by Empirical Bayes (EB). The 12 links that were identified by EB were identified as significant by HB modeling, illustrating agreement in results. Furthermore, HB analysis found 6 extra links. This implies that EB is a good approximation to HB and, hence, EB can be recommended to use when computation is challenging. In fact, in this analysis, HB took around 100 hours to converge, while it only took 10 hours to implement the EB approach. Another challenge for HB is the selection of a sensible prior that requires a thorough investigation. Although a flat or



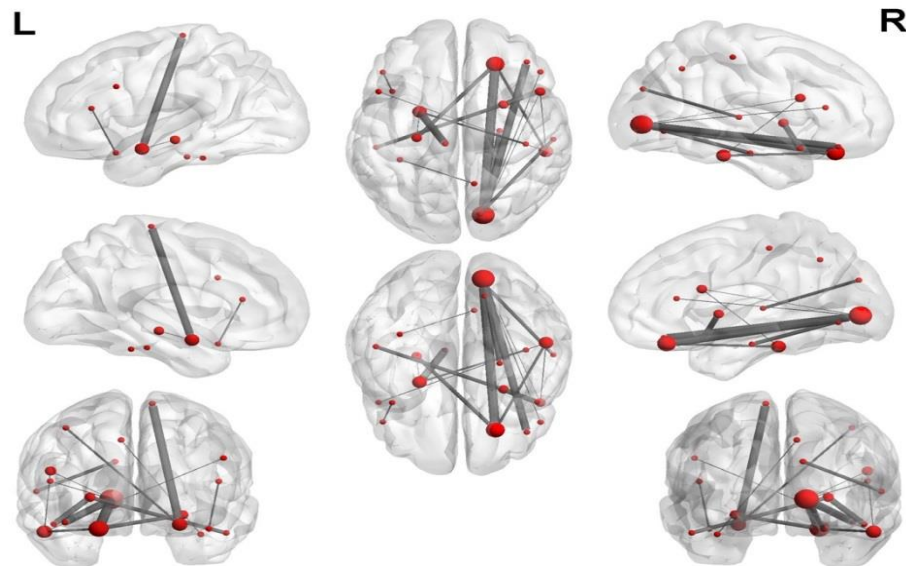


Figure 2: Brain Network from Bayesian Analysis

non-informative prior is usually recommended, in many cases a flat prior can be problematic. [15] and [17] indicated that in several instances non-informative priors can have undue impact on the posterior distributions.

As pointed out by [6], convergence of MCMC can be very difficult to diagnose as most of the usual diagnostic tools have drawbacks [7]. Moreover, with increasing computation power, WinBUGS takes care of hierarchical Bayesian model implementation in the background with high efficiency. As it is becoming easy to fit a complicated hierarchical Bayesian model with WinBUGS, statisticians tend to fit a hierarchical Bayesian model larger than the data can readily support. Given the pros and cons of EB and HB, the modeling choice depends on problem at hand. Fortunately, EB and HB lead to similar results in this analysis, ensuring the validity of the list of links that are significantly different in autism as compared with control.

4.5 Network of Analysis of Disrupted Connectivities

The Primary Auditory, Visual and Motor Cortices are a few to name that have significantly disrupted functional connectivities in the autism group compared to the control group. Using these disrupted connectivities, we constructed a network

analysis presented in Figure 2. Figure 2 reveals that Broadmann region Left Primary Auditory Cortex (61) of the ASD has disruptions with a total of six other Broadmann regions: the Right Primary Auditory Cortex (62), Right Subcentral Area (66), Right Dorsolateral Prefrontal Cortex (84), Right IFC Pars Triangularis (70), Right IFC Pars Opercularis (68), and Right Superior Temporal Gyrus (22). In addition, the Right Subcentral Area (66) and Insular Cortex (8) each have three disruptions. Some other isolated disrupted connectivities (on the top and top right side) are shown in this figure. A plausible interpretation of this network is that the disruption between the Primary Auditory Cortex and Subcentral Area may produce deflated verbal responses in the autism group due to poor performance of the Auditory Cortex. Similarly, disruptions between Primary Auditory Cortex and Right Dorsolateral Prefrontal Cortex (DLPFC) may have impact on the A-not B task, delayed response task and object retrieval task; in other words, autistic subjects may have difficulty holding onto information. Subjects with disrupted DLPFC may have problems identifying an object they have previously seen.

Table 4: Significant Links Detected by Hierarchical Bayesian Analysis

Number	Link	Mean Difference	P-Value
1	61-66	0.12401059	3.66E-05
2	61-62	0.11482648	6.85E-05
3	08-01	0.09312393	6.87E-05
4	14-54	0.08030308	0.000151718
5	61-68	0.10010339	0.000283524
6	14-27	0.06500111	0.000316542
7	07-66	0.0973133	0.000327247
8	57-82	-0.08345572	0.000409923
9	08-74	-0.08531813	0.000740115
10	20-38	0.0666724	0.000944472
11	25-77	0.07971842	0.001273403
12	61-70	0.07243045	0.00130313
13	61-84	0.08507215	0.001332772
14	22-61	0.08128412	0.001361554
15	65-66	0.10029997	0.001408855
16	07-08	0.12526509	0.00146067
17	22-61	0.08128412	0.001479168

5. Conclusion

Detection of disrupted connectivities in neuroimaging studies is an important problem for better targeting therapeutic interventions. The motivation for developing a hierarchical Bayesian model in this context is to incorporate within subject correlations in the analysis, as eluding of such correlations may produce biased results in the decision-making process. Several computational challenges are addressed while implementing the hierarchical Bayesian model. We have detected several disrupted connectivities after controlling the false discovery rate for reliability and robustness. Disrupted connectivities identified in autistic patients by the hierarchical Bayesian model match were also detected by the empirical Bayesian approach. As the network analysis shows that the Primary Auditory Cortex that has disrupted connectivities with several other regions, this may be the hub of disruption. Furthermore, the Insular cortex may be considered as a subhub of disruptions. These centers of disruptions may be used as target for applications of neurobehavioral interventions. The current analysis uses only resting state functional connectivity data. Results of structural connectivity (e.g. DTI) can be correlated with these findings for support of our understanding of how regions work together in the presence of strong or weak structural connections, referred to as effective connectivity.

Acknowledgement

We would like to thank the referees for their careful review and insightful feedback. The time they dedicated to this manuscript improved this work.

References

- [1] Aertsen, A., Gerstein, G. and Habib, M. (1989). Dynamics of neuronal firing correlation: modulation of effective connectivity. *J Neurophysiol* 61, 900.
- [2] APA (2000). *Diagnostic and statistical manual of mental disorders*. APA, Washington. DC.
- [3] Benjamini, Y. and Hochberg, Y. (1995). Controlling the false discovery rate: A practical and powerful approach to multiple testing. *Journal of the Royal Statistical Society. Series B (Methodological)* 57, 289–300.
- [4] Brooks, S. P. and Gelman, A. (1998). General methods for monitoring convergence of iterative simulations. *Journal of Computational and Graphical Statistics* 7, 434.

- [5] Carlin, B. P., Gelfand, A. E. and Smith, A. F. (1992). Hierarchical bayesian analysis of change point problems. *Journal of the Royal Statistical Society. Series C* 41, 389.
- [6] Carlin, B. P. and Louis, T. A. (2000). Empirical bayes: Past, present and future. *Journal of the American Statistical Association* 95, 1286.
- [7] Cowles, M. K. and Carlin, B. P. (1996). Markov chain monte carlo convergence diagnostics: A comparative review. *Journal of American Statistical. Association* 91, 883.
- [8] Fombonne, E. (1999). The epidemiology of autism: a review. *Psychol Med.* 29, 769.
- [9] Friston, K. and Frith, C. (1993). Functional connectivity: the principal-component analysis of large (pet) data sets. *J. Cereb. Blood Flow Metab.* 13, 5.
- [10] Gelman, A. and Rubin, D. B. (1992). Inference from iterative simulation using multiple sequences. *Statistical Science* 7, 457.
- [11] Geman, S. and Geman, D. (1984). Stochastic relaxation, gibbs distributions, and the bayesian restoration of images. *IEEE-PAMI* 7, 721.
- [12] Geweke, J. (1992). *Bayesian Statistics*. Oxford University Press, New York.
- [13] Good, I. (1965). *The Estimation of Probabilities: An Essay on Modern Bayesian Methods*. MIT Press, Cambridge.
- [14] Hastings, W. (1970). Monte carlo sampling methods using markov chains and their applications. *Biometrika* 57, 97.
- [15] Hodges, J. S. and Sargent, D. J. (2001). Counting degrees of freedom in hierarchical and other richly parameterised models. *Biometrika* 88, 367.
- [16] Metropolis, N. (1953). Equation of state calculations by fast computing machines. *J. Chem. Phys.* 14, 997.
- [17] Natarajan, R. and Kass, R. E. (2000). Reference bayesian methods for generalized linear mixed models. *Journal of the American Statistical Association* 95, 449.
- [18] Ntzoufras, I. (2009). *Bayesian Modeling Using WinBUGS*. Wiley, New Jersey.